

Potential degradation products of abemaciclib: Identification and structural characterization employing LC-Q/TOF-MS and NMR including mechanistic explanation

Nachiket Kathar, Niraj Rajput, Tarang Jadav, Pinaki Sengupta *

Department of Pharmaceutical Analysis, National Institute of Pharmaceutical Education and Research-Ahmedabad (NIPER-A), An Institute of National Importance, Government of India, Department of Pharmaceuticals, Ministry of Chemicals and Fertilizers, Opp. Airforce Station, Palaj, Gandhinagar 382355, Gujarat, India

ARTICLE INFO

Keywords:
Abemaciclib
Degradation products
Characterization
LC-Q/TOF-MS and ^1H NMR
Stability indicating analytical method
In silico toxicity

ABSTRACT

Degradation products are the potential drug impurities that can be generated during transport and storage of pharmaceuticals. Before this study, degradation chemistry and potential degradation products of abemaciclib (ABM) were unknown. Moreover, no stability-indicating analytical method was available that can be used to analyse ABM in presence of its degradation products. In this study, stress testing on ABM was carried out under oxidative, thermal, photolytic (UV & visible), and hydrolytic (acid, alkaline, and neutral) degradation conditions. The study revealed that ABM is susceptible to photolytic, oxidative, and thermal stress leading to the formation of five degradation products (DPs). ABM and its degradation products were chromatographically separated employing a developed RP-HPLC-based stability-indicating analytical method. The method was transferred to an LC-Q-TOF system for further analysis. To elucidate the structure of degradation products, fragmentation pathway of ABM was initially established through high-resolution mass spectrometry (HRMS). Subsequently, mass fragmentation pathways of all the DPs have been established through HRMS and MSⁿ based analysis. The major degradation product was isolated and fully characterized using atmospheric chemical ionization-mass spectrometry and nuclear magnetic resonance techniques. ABM showed extensive degradation under oxidative and photolytic systems. Therefore, special care may be sought during storage and transport of ABM or its formulations to avoid photolytic and oxidative stress exposure to the drug. Lastly, *in silico* toxicity of the characterized degradation products was assessed employing ProTox II online web predictor freeware in which some of them were found to have the potential of hepatotoxicity, immunogenicity and mutagenicity.

1. Introduction

Abemaciclib (ABM) was approved by United States Food and Drug Administration (USFDA) as an antineoplastic agent in 2017 for the treatment of human epidermal growth factor receptor 2 (HER2)-negative and hormone receptor (HR)-positive metastatic or advanced breast cancer. Chemically, it is N-[5-[(4-ethylpiperazin-1-yl) methyl] pyridin-2-yl]- 5-fluoro-4-(7-fluoro-2-methyl-3-propan-2-yl benzimidazol-5-yl) pyrimidin-2-amine (Fig. 1). In general, cancer cell proliferation progresses through cell cycle dysfunction. Retinoblastoma (Rb) is a cancer suppressor protein that restricts the cell cycle in between transition from G1 to S phase. Phosphorylation of this protein by cyclin-dependent kinases (CDK 4 & 6) leads to dysregulation of the cell cycle and

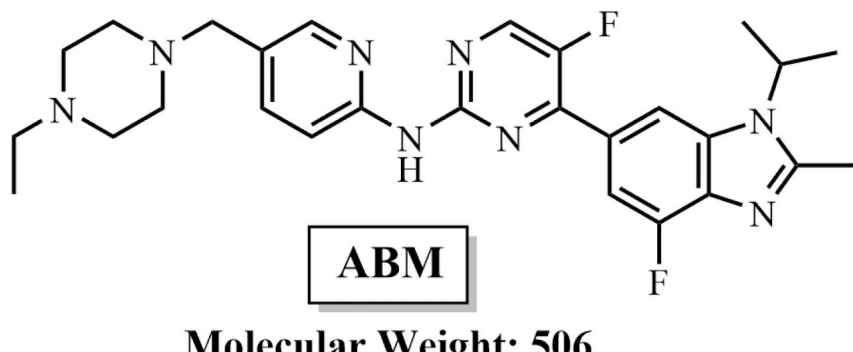
hyperproliferation of cancer cells. ABM indirectly restricts phosphorylation of the Rb proteins through its dual inhibitory effect on the CDK 4 and 6 enzyme complex, which further leads to cell cycle arrest in the G1 phase and limits cancer cell growth [1–4].

The stability of pharmaceuticals is an utmost concern of the pharmaceutical industry, as they may degrade when exposed to various environmental stimuli such as light, oxygen, humidity, pH, temperature, etc. during transport and storage. Such degradation products are the potential drug impurities that can be generated during storage of pharmaceuticals. This phenomenon can lead to the production of medicines with compromised quality and safety profiles due to the unknown toxicities of degradation products. Regulatory authorities including USFDA suggests continuous monitoring of pharmaceuticals through

* Correspondence to: National Institute of Pharmaceutical Education and Research-Ahmedabad (NIPER-A), An Institute of National Importance, Government of India, Department of Pharmaceuticals, Ministry of Chemicals and Fertilizers, Opp. Airforce Station, Palaj, Gandhinagar 382355, Gujarat, India.

E-mail address: psg725@gmail.com (P. Sengupta).





Molecular Weight: 506

Fig. 1. Structure of ABM.

various stability testing methodologies and also provide specific limits to control these impurities. A forced degradation study is one of the methods used to test the stability of pharmaceuticals by exposing them to different stress conditions and generating all possible degradants in less time. It provides a straightforward insight into understanding structural weak points in the drug, which further motivates the development of drugs with improved chemical stability. Stress studies also help to determine proper storage and packaging conditions for pharmaceuticals after the batch has been released to the market. ICH has published a list of guidelines, including ICH Q1A and Q1B, to perform stress studies on pharmaceuticals under different environmental conditions such as photolytic (ICH Q1B), oxidative, thermal, and hydrolytic (acid, base, and neutral) (ICH Q1A) [5–16]. These samples are further utilised to develop a stability-indicating analytical method (SIAM) to evaluate the stability of pharmaceuticals. Characterization of degradation products is important to understand the mechanism behind the degradation, and it also helps to predict its toxicity based on structural alerts if present. Several modern analytical techniques, such as nuclear magnetic resonance (NMR), high-resolution mass spectrometry (HRMS), X-ray crystallography, and Fourier transform infrared (FTIR) spectroscopy are employed for determining the exact structure of degradation products. Isolation of degradation products is important as it permits a more detailed examination of molecular structure with several orthogonal techniques. These isolated impurities are also used as a standard in the stability-indicating method as a part of the daily quality control process.

In a study, Kadi et al. have identified in vitro reactive metabolites of ABM by using HRMS technique [17]. Turković et al. reported a study to quantify ABM with palbociclib, ribociclib, anastrazole, letrozole, and fulvestrant in human plasma by using LC-MS/MS technology [18]. Sharmila et al. reported another study on the quantification of abemaciclib in human plasma employing LC-MS/MS [19]. To the best of our knowledge, no such report has been published on understanding the degradation chemistry of ABM under various stress conditions till date. Moreover, no SIAM is available to monitor the stability of ABM during its storage, transport, and packaging. Therefore, a detailed investigation of the degradation chemistry of ABM was carried out in the present study. The experimental work was performed following available ICH guidelines. ABM was exposed to different stress conditions. Stressed samples were used for developing the SIAM and to study mass fragmentation behaviour of the degradants through LC-QTOF system to establish their fragmentation patterns. A mechanistic explanation was employed to justify the structure of the DPs. An *in silico* toxicity assessment of the drug and its DPs was carried out using ProTox II software.

2. Experimental conditions

2.1. Chemicals and reagents

ABM (Purity, more than 99%) was procured from Clearsynth Labs Ltd. Mumbai, Maharashtra. Analytical reagent (AR) grade ammonium formate obtained from Sigma Aldrich (Mumbai, India) was used to prepare buffer solution for HPLC and LC-MS analysis. Thermo Fisher Scientific Pvt. Ltd. (Maharashtra, India) supplied acetonitrile (ACN) (HPLC and LC-MS grade), sodium hydroxide (NaOH), hydrogen peroxide (H₂O₂), and hydrochloric acid (HCl). AR grade formic acid (HCOOH) was supplied by Fisher Chemicals (Maharashtra, India), which was used to adjust pH of mobile phase. Ultrapure water was used during the entire study for preparing dilutions and buffers were supplied from in-house Millipore Milli Q assembly (Millipore, USA).

2.2. Apparatus and equipment

Photolytic studies were performed following option 2 of the ICH Q1B (guideline for photostability testing of new drug substance and drug products) using a photostability chamber (Newtronic Lifecare, Maharashtra, India) equipped with white fluorescence lamp and UV lamp in separate chambers. Hydrolytic and thermal degradation experiments were carried out using a hot air oven (Heratherm, Thermo Scientific Pvt. Ltd. Hyderabad) under controlled temperature. A pH meter (Eutech instruments, Haryana, India) was employed to record and adjust the pH of mobile phase during method development and analysis. A calibrated microbalance (Mettler-Toledo, Maharashtra, India) was employed to weigh the samples. A sonicator (Labman scientific instruments, Maharashtra, India) was used for mobile phase degassing and to dissolve samples. All stressed degraded samples were analyzed by using an Agilent 1260 infinity II series HPLC (Agilent Technologies, USA) consisting of a diode array detector (DAD) (G7115A), a vial sampler (G7129A) equipped with a thermostat, and dual piston quaternary pump (G7111B).

The MS and MS/MS data were obtained through a liquid chromatography-quadrupole time of flight (LC-Q-TOF) system (Agilent Technologies, USA). The LC-part of the instrument comprised of Agilent's 1290 Infinity ultra-high performance liquid chromatography (UHPLC) system equipped with a DAD detector (G7117A), temperature-controlled column compartment (G7116B), a multisampler (G7167B), and dual piston quaternary pump (G7104A). The MS part of the instrument comprised of Agilent 6545 Q-TOF system which had electrospray ionization (ESI) as a source. For the interpretation of mass spectrometric data, Agilent Mass Hunter workstation software (version B.07.00) was employed. MS³ analysis was performed by using a quadrupole ion trap of Sciex QQQ-trap 6500 + system (Sciex, MA, USA) equipped with electrospray ionization as ionizing source. The ¹H NMR spectrum of the drug and DP2 were obtained using a Bruker 500 MHz

NMR instrument. Deuterated-dimethyl sulfoxide (DMSO-D6) was used as a diluent, and tetramethylsilane (TMS) was used as a reference standard. All chemical shift values were represented in parts per million (ppm) unit scale.

2.3. Stress study

Hydrolytic, oxidative, and thermal stress studies on ABM were performed in compliance with the ICH Q1A (R2) guideline, whereas photolytic degradation studies (UV and visible) were conducted by following the ICH Q1B guideline. For hydrolytic and oxidative stress, the study was conducted in solution form, while for photolytic degradation, it was carried out in both solid (as a thin layer) and solution forms of the drug. For the thermal degradation study, only the solid form of the drug was used. As ABM was sparingly soluble in water, to resolve this a diluent having a mixture of ACN and water in the ratio of 70:30%v/v was used during the entire study. Hydrolytic studies were performed under different pH conditions, including 1&2 mol/L HCl for acidic, 1&2 mol/L NaOH for basic, and a mixture of 50:50%v/v water: diluent for neutral stress. The temperature and duration for all hydrolytic studies were optimized at 60 °C and 72 h, respectively. The oxidative degradation studies were conducted with different percentages of H₂O₂ (0.05%, 0.1%, 0.3%, 1%, and 3%) at ambient temperature in the dark to avoid any interference due to light. A negative oxidative control solution was also prepared, containing the same concentration of the drug without the inclusion of a stressor. For photolytic degradation studies, ABM was exposed to UV and visible light in a photolytic chamber operated as per option B of the ICH Q1B guideline. The drug was exposed to 3 individual cycles of UV (1.2 million lux-h) and visible (200 Watt.h/m²) light at 40 °C and 75% RH. Negative control samples (petri plates wrapped with aluminum foil) were also placed in parallel inside the photostability chamber under similar conditions as the test samples. After each cycle, the samples were collected and subsequently dissolved (in the case of solid samples) or diluted (in the case of liquid samples) for subsequent analysis using an HPLC system. ABM was subjected to dry heat in a petri dish at 80 °C for seven days with a negative control (petri dish wrapped with aluminum foil) in a hot air oven as part of a thermolytic degradation study. For all liquid state degradation studies, the concentration of drug used was 500 ppm, which was prepared with a 50:50%v/v ratio of diluent and the respective stressor. During each study, at different time intervals, sample aliquots were collected and diluted five times with 70:30%v/v ACN:water for HPLC analysis. Table S1 depicts the different optimized stress conditions employed to degrade ABM.

2.4. SIAM development and optimization

An RP-HPLC based SIAM was developed to effectively separate and quantify ABM in presence of its all DPs in different stress samples. Multiple column chemistries were assessed to get optimum retention and resolution between ABM and its DP's. Among them, Agilent's Zorbax eclipsed plus C18 column with a dimension of 250 mm × 4.6 mm ID, 5 µm particle size, demonstrated better resolution and retention. Different buffers such as formic acid, ammonium formate and ammonium acetate were checked to get good peak shape and resolution. Ammonium formate was selected as a buffer of choice as it provided optimum chromatographic resolution and peak shape. To optimize RP-HPLC method, different chromatographic parameters such as proportion of buffer and organic modifier (ACN), buffer pH and flow rate were used. The final method was developed with mobile phase having a mixture of 10 mM ammonium formate (pH 3.6) (Component A) and ACN (Component B), in gradient elution mode. A gradient program having the percent ratio of mobile phases (A:B) of 80:20 for initial 3 min, 70:30 upto 8 min, 60:40 upto 13 min, 30:70 upto 14 min, 10: 90 upto 16 min, and 80:20 till 20 min was employed. Other chromatographic parameters like detection wavelength, injection volume, and flow rate

were used to be 300 nm, 10 µL, and 1 mL/min respectively. A system suitability test (SST) was carried out at 100 ppm concentration of the drug (n = 6), to evaluate standard SST parameters like capacity factor, retention time (RT), tailing factor, and, theoretical plates.

2.5. Validation of SIAM

The ICH Q2R1 guideline was used to validate the aforementioned analytical method. The linearity of the developed method was assessed in triplicate (n = 3) in the range of 20–160 ppm and correlation coefficient (r^2) value was calculated by plotting the calibration curve. Standard deviation of the response and the slope of calibration curve was used to determine the limit of detection (LOD) and limit of quantitation (LOQ). Six replicate injections at LOD and LOQ values were injected, and %RSD of average area was calculated. The developed SIAM was tested for intra-day precision by injecting ABM solution in triplicates (n = 3) at 80%, 100%, and 120% of the test concentration (100 ppm). Similarly, inter-day precision was checked by conducting the experiment over two consecutive days, injecting the same concentration (80%, 100% and 120%) in triplicate (n = 3). The accuracy of the method was performed at three different concentrations 80%, 100% and 120% of test concentration (100 ppm) in triplicate (n = 3) and recovery was determined by back calculating the average area through the calibration curve. To test the specificity of the method, various samples were injected, including the blank (diluent), placebo (consisting of silicon dioxide, lactose monohydrate, sodium stearyl fumarate, croscarmellose sodium, microcrystalline cellulose 102 and 101, and talc), standard ABM solution (100 ppm), and ABM solution with excipients. The excipients used in specificity study were selected as per the marketed formulation of ABM (verzenios tablet). The chromatograms of these samples were compared, and any interference at the RT of ABM was examined. Robustness of the developed method was evaluated by making slight modifications in pH of mobile phase and flow rate of the method.

2.6. LC-MS/MS and MS³ studies

MS and MS/MS data were acquired for the stressed samples employing the same gradient program and mobile phase contents. The analysis was done at a flow rate of 0.5 mL/min employing 5 µL injection volume and 10 ppm concentration. A C18 column selected for the analysis was having 100 mm length and 4.6 mm ID with a particle size of 2.7 µm (Agilent's Poroshell SB C18). Mass spectrometric (MS) data were acquired in positive ESI (+ve ESI) mode covering a range of 50–1000 Da. Highly pure nitrogen (N₂) was used as drying gas and sheath gas at flow rate and temperature of 8 L/min at 320 °C and 11 L/min at 300 °C respectively. Tuning of MS parameters revealed optimal sensitivity with 45 eV collision energy, 175 V fragmentor voltage, and, 65 V skimmer voltage. The mass isolation width was set to ~ 4 m/z (medium). The LC-MS data was collected sequentially through the system. Initially, ABM was subjected to an MS scan for determining m/z value and its prominent fragments. Subsequently, an MS/MS experiment was performed to gain a comprehensive knowledge of fragmentation behavior of the drug, aiding in the establishment of a fragmentation pattern for ABM. Following this, LC-MS spectra were similarly acquired for each sample. Firstly, MS data were acquired, followed by MS/MS data for each DP, enabling the establishment of their respective fragmentation pathways. Fragmentation pattern of ABM served as a guide for establishing fragmentation pattern of DPs. To assess the accuracy of the proposed fragmentation pathways, the mass ppm error was determined for all significant fragments obtained from MS/MS experiments. The acceptance criteria for mass ppm error was set at not more than 5 ppm. The MS³ analysis was carried out with collision energies of 30 eV (for DP1) and 50 eV (for DP2 to DP5), curtain gas (N₂) at 40 psi, spray voltage at 5 kV, declustering potential and entrance potential at 50 V and 10 V, respectively. Ion spray voltage was set at 40 V. Excitation energies

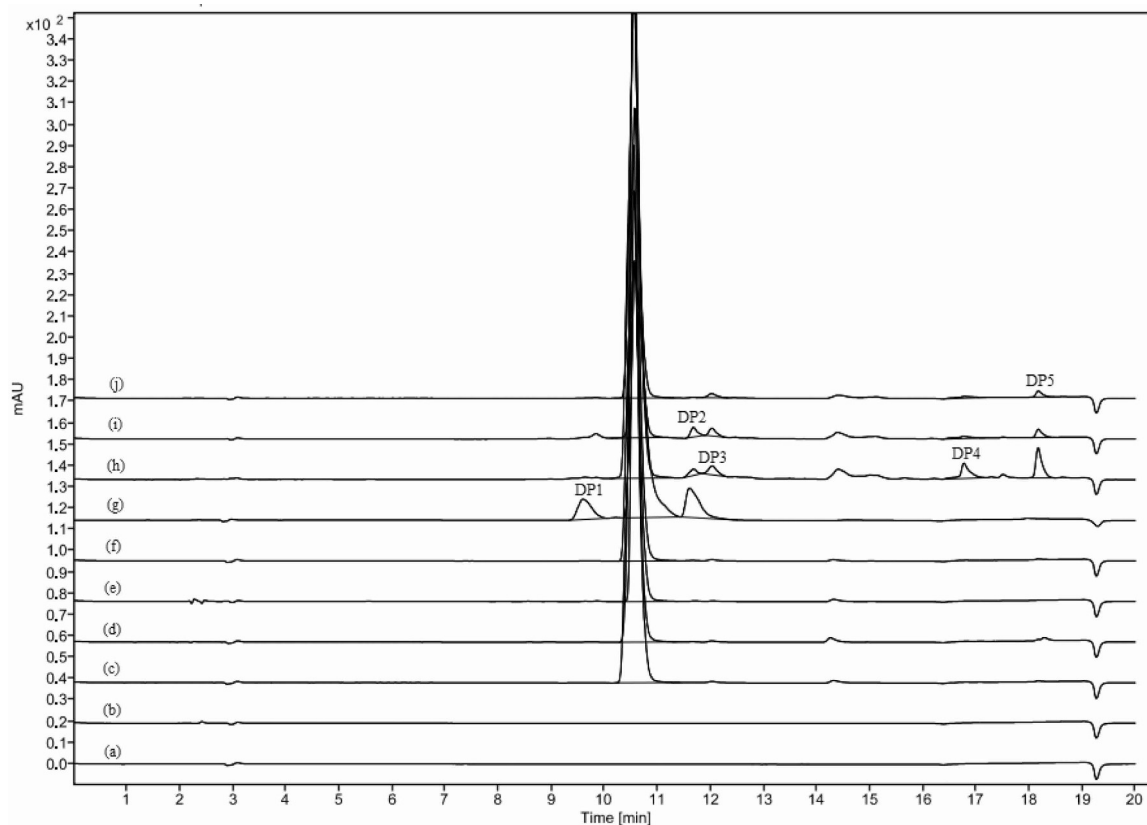


Fig. 2. Overlay of chromatograms generated from different stress study samples a) 0 hr Blank, b) 0 hr 0.05% H_2O_2 , c) 0 hr 100 ppm ABM, d) Day 7 acid stressed sample, e) Day 7 base stressed sample, f) Day 7 neutral stressed sample, g) 3 hr oxidative stressed sample, h) 3rd cycle UV stressed sample, i) 3rd cycle Visible light stressed sample, and, j) Day 7 thermolytic stressed sample.

AF2 and AF3 were set at 0.4 and 1.38–2.87, respectively.

2.7. APCI based characterization of DP2

Distinguishing N-oxide and hydroxylated degradation product based on ESI-MS/MS spectrum (low energy) is difficult if both changes occur on the same ring of the molecule. Since N-oxides are not stable at a higher temperature, DP2 was subjected to ionization in positive atmospheric pressure chemical ionization (+ve APCI) for getting characteristic $\text{M}+\text{H}-16$ ($\text{M}+\text{H}+\text{O} \rightarrow \text{M}+\text{H}-\text{O}$) peak in MS spectrum of DP2 due to its thermal de-oxygenation [20,21]. The optimized APCI-QTOF MS parameters for the above analysis are provided in Table S2.

2.8. Isolation and characterization of DP2 by ^1H NMR

DP2 was isolated using the same HPLC system applied for developing SIAM. The column utilized for isolation was an Agilent Zorbax Eclipsed plus C18 column (250×4.6 mm, $5 \mu\text{m}$). A new 16 min isocratic method was developed with a mobile phase composition of 80% A (ammonium formate (10 mM), pH 3.6) and 20% B (ACN). The injection volume and flow rate was set to be $90 \mu\text{L}$ and $1 \text{ mL}/\text{min}$ respectively. The UV-Vis detector was set at a fixed wavelength of 300 nm to identify DP2 during isolation. 5 mg of ABM was subjected to oxidative stress (3% H_2O_2) for 1 h at RT followed by 2 days layophilization to remove the remaining H_2O_2 from the reaction mixture before isolation through HPLC. During isolation, the eluent fraction corresponding to DP2 peak was collected and verified in subsequent runs. All fractions were combined and heat dried using a Buchi R-300 rotary evaporator (Switzerland). The dried sample was dissolved in CDCl_3 , with TMS serving as the internal standard, and subjected to ^1H NMR analysis.

2.9. In silico toxicity prediction of ABM and its DPs

Structural alteration in a drug's structure during its shelf life may lead to the generation of DPs having distinct structural features than drug with undesired pharmacological effects. To avoid any toxicity concerns with DP, it is important to perform *in silico* toxicity prediction as part of the drug development program. ABM and its degradation products were subjected to *in silico* toxicity prediction using ProTox II toxicity predictor freeware. The predicted toxicity profile of the drug was compared with the toxicity profiles of individual DP. The molecular details of different DPs were used to forecast their toxicities and generated statistical comparisons based on the known toxicity of reference molecules. Moreover, a confidence score was assigned to each DP by the software based on toxicity prediction. If the confidence score exceeded 70% (0.7), the software considered the toxicity to be severe.

3. Results and discussion

ABM (Fig. 1) was eluted out at a retention time of 10.5 min on a newly developed SIAM, having a total run time of 20 min. Before each analysis, system suitability parameters were assessed to ensure compliance with chromatographic acceptance criteria. All system suitability parameters, including theoretical plates (N), capacity factor (k), and peak asymmetry factor were ascertained to be > 2000 , < 6 , and < 1.2 , respectively.

3.1. Different stress conditions

3.1.1. Hydrolytic degradation

The acidic hydrolytic data of ABM demonstrated that the drug was stable in 1 M HCl at 60 °C for 72 h. To further assess the drug's stability,

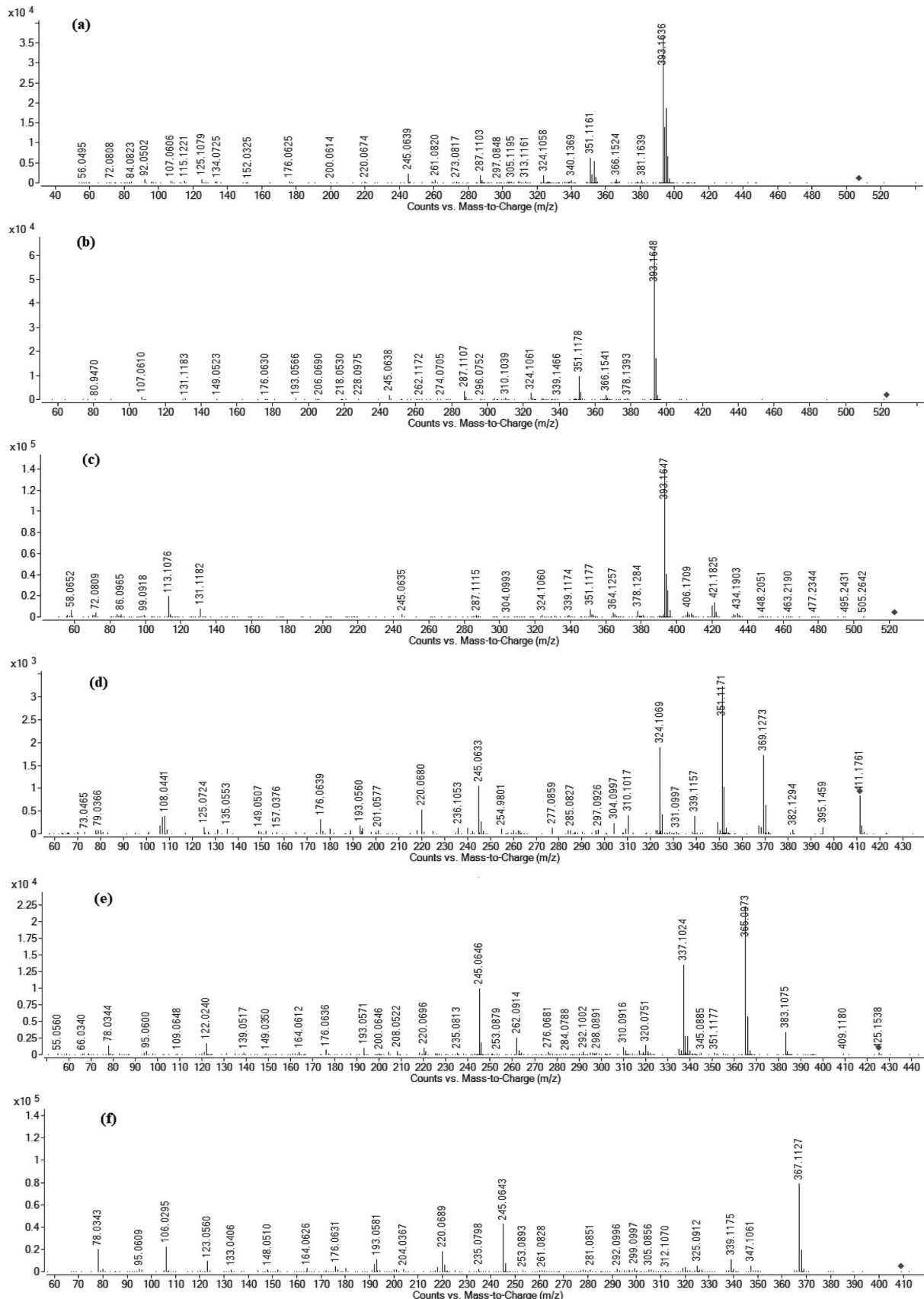


Fig. 3. ESI-MS/MS spectra of a) ABM, b) DP1, c) DP2, d) DP3, e) DP4, and f) DP5.

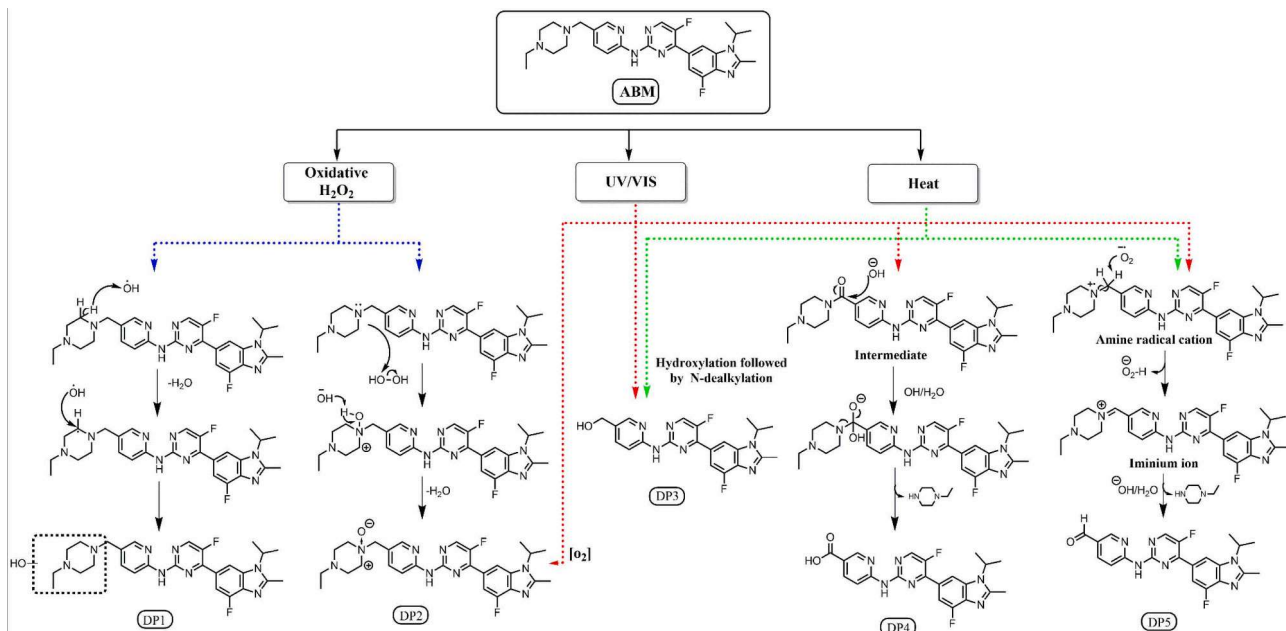


Fig. 4. Possible molecular mechanism behind formation of DPs.

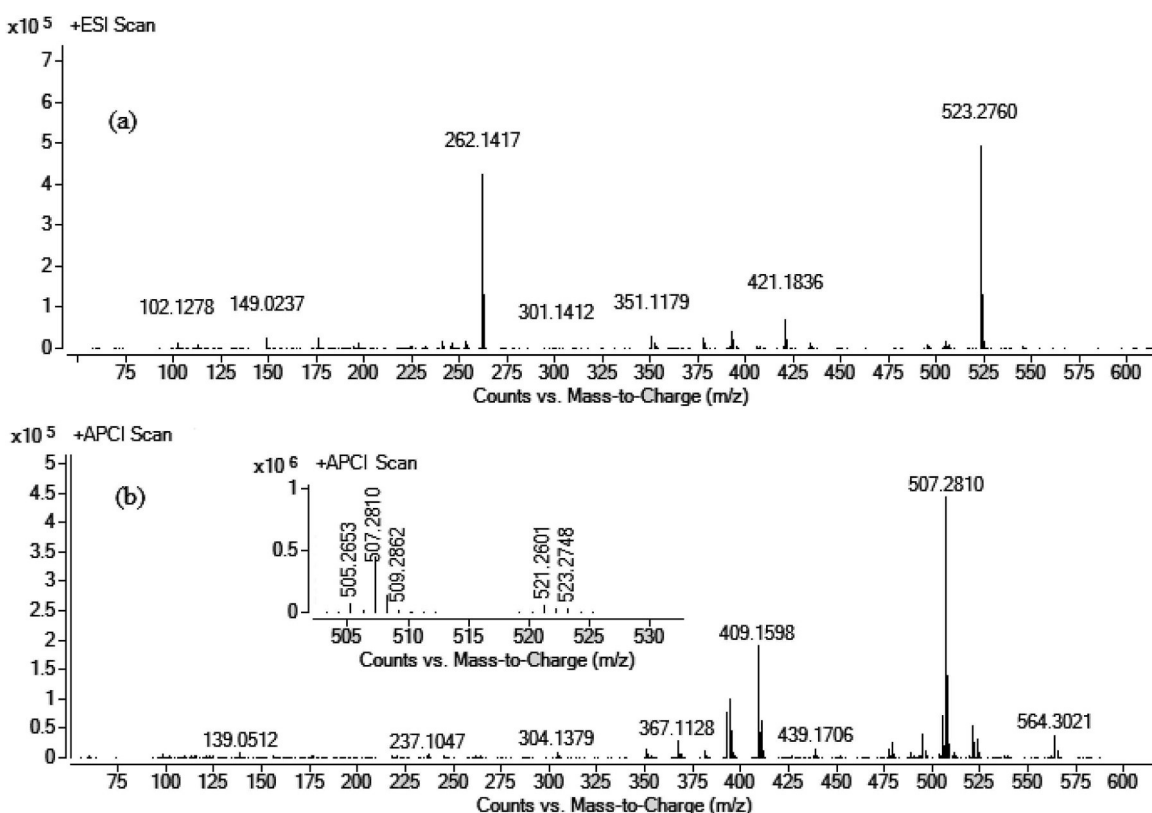


Fig. 5. Comparison of MS spectrum of DP2 a) ESI-MS, b) APCI-MS.

the study was repeated under more rigorous conditions by increasing the concentration of the stressor to 2 mol/L at 60 °C for 72 h. Even under this condition, no degradation of ABM was observed which indicated its stability under acidic hydrolytic conditions 9 (Fig. 2d). Fig. 2(a-j) shows representative chromatograms of the degradation study samples of ABM subjected to various stress conditions. Hydrolytic study in alkaline conditions was conducted with 1 M and 2 M NaOH at 60 °C for 72 h. No degradation of ABM was observed in alkaline conditions (Fig. 2e).

Furthermore, ABM demonstrated stability during neutral hydrolysis at 60 °C, showing no additional peak after 72 h (Fig. 2f). For all hydrolytic studies, peak area of the drug was compared with zero hour control samples to assess the formation of any DP which do not have UV absorbance. In Fig. 2, tiny peaks between RT 14–15 min were present in the sample before performing stress studies. As these peaks were not degradation products, we have not considered them for characterization.

Table 1
¹H NMR data of ABM and DP2.

Atom number	ABM δ _H (ppm), multiplicity	DP 2 δ _H (ppm), multiplicity
1	8.46-8.47 (d, 1H)	8.46-8.47 (d, 1H)
3	7.70-7.72 (dd, 1H)	7.68-7.70 (dd, 1H)
4	7.81-7.83 (d, 1H)	7.81-7.83 (d, 1H)
7	3.52 (s, 2H)	3.62 (s, 2H)
9 (-NH)	8.32 (s, 1H)	8.22 (s, 1H)
14	8.40-8.42 (d, 1H)	8.43-8.45 (d, 1H)
18	8.22-8.22 (d, 1H)	8.20-8.20 (d, 1H)
22	8.28-8.28 (d, 1H)	8.28-8.28 (d, 1H)
26	4.72-4.80 (h, 1H)	4.73-4.80 (h, 1H)
27,28	1.73-1.74 (d, 6H)	1.73-1.75 (d, 6H)
29	2.72 (s, 3H)	2.72 (s, 3H)
31, 35	2.46-2.66 (m, 8H)	3.51-3.57 (4H)
32		3.26-3.30 (t, 2H)
34		3.06-3.10 (t, 2H)
36	2.42-2.46 (q, 2H)	2.26-2.29 (q, 2H)
37	1.09-1.12 (t, 3H)	0.89-0.92 (t, 3H)

3.1.2. Oxidative degradation

Oxidative stress study data on ABM with 3% H₂O₂ as a stressor at room temperature demonstrated extensive degradation of the drug in this condition. To get the optimum degradation, the study was repeated with 1%, 0.3%, 0.1%, and 0.05% H₂O₂. The data revealed optimum oxidative degradation of the drug with 0.05% H₂O₂, leading to the formation of two degradation products, DP1 (~6.5%) and DP2 (~9%), at 3 h (Fig. 2g). Both degradation products were observed to increase over the period of 24 h without forming any new DP.

3.1.3. Photolytic degradation

Solid and liquid form of the drug was exposed to light (UV and Visible) following ICH Q1B guideline. The chromatographic data of photolytic sample in both phases showed formation of four DP2, DP3, DP4 and DP5 (Fig. 2h and 2i). All four DPs were observed in UV stress (3 cycles of 200 watt.h.m⁻²) samples at area percent of DP2: ~1.2%; DP3: ~1.5%; DP4: ~1.7%; and DP5: ~3.2%; whereas in visible light stress (3 cycles of 1.2 million lux.h) the percentage degradation of drug was found to be less.

3.1.4. Thermal degradation

A thermal degradation study was conducted at 80 °C in a hot air oven over the period of 7 days. The chromatographic data indicated slight degradation of ABM (~2.5%) under thermal stress conditions on 7th day with the formation of same DP3 and DP5 that was formed under photolytic conditions (Fig. 2j).

3.2. Method validation

The r² value of the linearity curve was found to be 0.9999, suggesting a linear response across the chosen concentration range. The LOD and LOQ values for the developed SIAM were found to be 1.6 ppm and 4.95 ppm, respectively. Percent RSD of average area in six replicates (n = 6) at LOD and LOQ values was less than 2%. Intra-day precision, evaluated for two batches, and inter-day precision, assessed over two consecutive days (three batches), both demonstrated %RSD values

below 2%, confirming the precision and reliability of SIAM (Table S3 and S4). The accuracy was found in terms of % recovery of ABM. Recovery (%) at three different concentration levels 80%, 100%, and 120% of test concentration was found to be 99.40, 100.62, and 99.85, respectively, indicating the accuracy of the developed analytical method (Table S5). Specificity data confirmed that there was no interference at the drug's RT from any excipient (Supplementary Fig. S1). The results of robustness study were within an acceptable range, showing the robustness of the developed analytical method.

3.3. LC-QTOF analysis

3.3.1. Fragmentation behaviour of ABM

As depicted in Fig. 2c, the retention of ABM was found to be 10.5 min. Supplementary figure 2 depicts ESI-MS spectrum of ABM and five DPs. The detailed ESI-MS/MS spectra of ABM are depicted in Fig. 3a, revealing the presence of quasi molecular ion peak at m/z 507.2796 [M+H]⁺ along with a base peak at m/z 393.1634 [M+H]⁺. MS/MS data was employed to investigate the fragmentation pattern of ABM, aiming to comprehend the drug's fragmentation behavior and subsequently reveal the structures of its DPs (Supplementary Fig. S3). The fragmentation behaviour of ABM shows breaking of precursor ion m/z 507 into many different product ions (m/z 393, 287, 366, 351, 324, 245, 176, 115, 92). The m/z 393 was produced from parent ion with the loss of the ethyl piperazine (C₆H₁₄N₂⁺) moiety through heterolytic cleavage of C-N bond. Furthermore, the prop-1-ene (C₃H₆) was lost during the generation of the ion with m/z 351 from m/z 393 with two possible structures including subsequent intramolecular cyclization to form 2 H-azepine ring. The ion with m/z 393 was further fragmented to m/z 366 via removal of HCN molecule. The m/z 324 was produced due to loss of the prop-1-ene from m/z 366 by heterolytic cleavage; subsequently, it produced the product ion m/z 176 by breaking the bond between the pyrimidine ring and benzo-imidazole ring. Next, a fragment ion with m/z 245 was produced from both m/z 287 and m/z 351 by the removal of the prop-1-ene and 5-methylpyridine-2-amine through heterolytic cleavage, respectively. A fragment with m/z 115 (ethyl piperazine) was formed from parent ion by losing C₂₁H₁₈F₂N₆. One more fragment with m/z 92 was generated from m/z 393 via loss of CH₁₃F₂N₅.

3.3.2. Fragmentation behaviour and mechanism behind formation of DPs

LC-MS/MS experiment was conducted with same chromatographic conditions for ABM and its DPs generated through various stress studies. Table S6 illustrates exact mass, practically observed mass, calculated mass ppm error and major m/z fragments of ABM and its DPs. Figs. 3 and 4 depicted the ESI-MS/MS spectra of ABM and all its DPs.

3.3.2.1. Oxidative DP (DP1). The DP1 was obtained from the oxidative degradation of ABM (Fig. 2g), which was eluted at an RT of 9.5 min. After analyzing the oxidative degradation sample by LC-MS/MS, it shows a molecular ion peak with m/z 523 [M+H]⁺ (Fig. 3b) which represents the mass difference of 16 Da from the drug mass due to hydroxylation at the piperazine ring (Table S6). MS/MS spectra of DP1 represented various product ions with m/z 523, 393, 366, 351, 324, 287, 245, 176, 131, and 107 (Supplementary Fig. S4). DP1 shows a similar fragmentation pattern as that of ABM. The only difference in fragmentation of DP1 from ABM was the formation of a fragment with m/z 131 instead of 115 (Supplementary Fig. S3) from molecular ion due to the neutral loss of C₂₁H₁₈F₂N₆ indicated hydroxylation of ethyl piperazine moiety. All fragment ion (Supplementary Fig. S4) produced from m/z 393 (m/z 366, 351, 324, 287 & 245) and m/z 131 (m/z 113 due to water loss) were confirmed through MS³ analysis of DP1 (Supplementary Fig. S9a & b). Since the mass ppm error computed for DP1 and its fragments were less than 10 ppm, the possible elemental composition of DP1 was postulated to be C₂₇H₃₃F₂N₈O⁺. The mechanism behind the formation of DP1 can be explained as radical based hydroxylation of

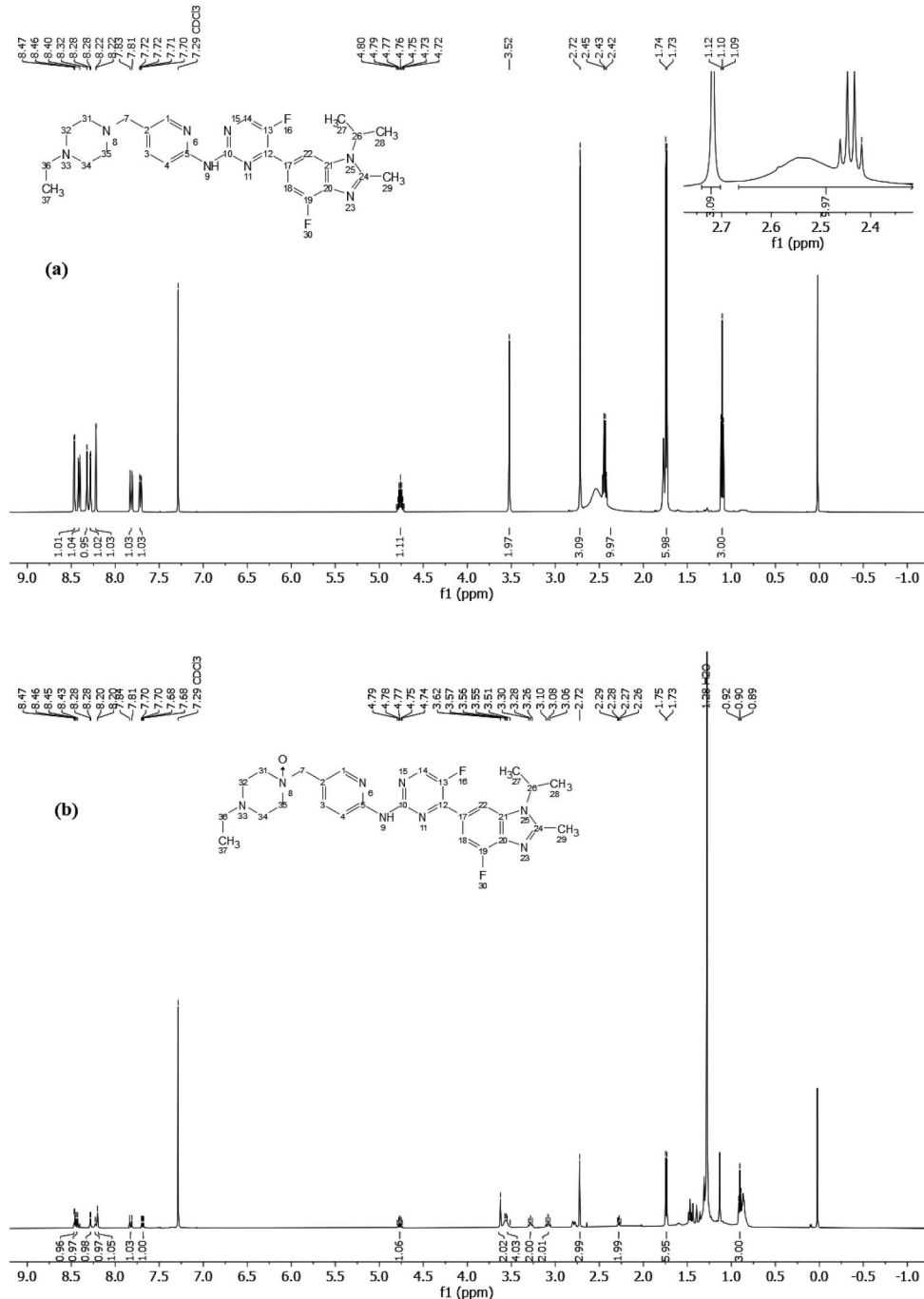
Fig. 6. ^1H NMR spectrum of a) ABM and b) DP2.

Table 2
In silico toxicity prediction chart.

Name	Toxicity class	Predicted LD50 value (mg/kg)	Toxicity prediction with confidence interval (CI)				
			Hepatotoxicity	Carcinogenicity	Immunotoxicity	Mutagenicity	Cytotoxicity
Drug	4	2000	Inactive (63%)	Inactive (61%)	Inactive (59%)	Inactive (60%)	Inactive (53%)
DP1	4	2000	Inactive (63%)	Inactive (56%)	Active (69%)	Inactive (65%)	Inactive (58%)
DP2	4	2000	Inactive (66%)	Inactive (53%)	Active (87%)	Active (50%)	Inactive (62%)
DP3	4	2000	Active (55%)	Inactive (50%)	Inactive (87%)	Active (55%)	Inactive (68%)
DP4	4	2000	Active (66%)	Active (50%)	Inactive (97%)	Inactive (53%)	Inactive (66%)
DP5	4	2000	Active (62%)	Inactive (59%)	Inactive (68%)	Active (68%)	Inactive (76%)

alpha carbon in presence of hydrogen peroxide, leading to the formation of 1-ethyl-4-((6-((5-fluoro-4-(4-fluoro-1-isopropyl-2-methyl-1 H-benzo[d]imidazol-6-yl) pyrimidin-2-yl) amino) pyridin-3-yl) methyl) piperazine-2-ol as DP1 (Fig. 4) [11]. Kalaria et al. reported their study on characterization of degradation products of ketorolac tromethamine using LC-QTOF system. Their study reported the same mechanism for the formation of dual hydroxylated DP of ketorolac tromethamine [22]. Rajput et al. have also published a study on characterization of degradation products of binimetinib using LC-MS/MS and NMR. In this article, the author has discussed a similar mechanism behind formation of hydroxylated DP [9].

3.3.2.2. Oxidative DP (DP2). The RT of DP2 was found to be 11.5 min during HPLC analysis (Fig. 2g). After performing its MS/MS analysis, molecular ion peak for DP2 was observed at m/z 523 indicating mass difference of 16 Da from ABM mass (m/z 507) (Fig. 3c). According to MS/MS data, the possible elemental composition for DP2 was found to be $C_{27}H_{33}F_3N_8O^+$, with a mass ppm error of less than 10 ppm (Table S6). The MS/MS data of DP2 revealed a fragment with m/z 505 formed from parent ion with loss of one H_2O molecule. Furthermore, the MS/MS data also revealed presence of other fragments with m/z 523, 505, 477, 421, 393, 287, 351, 324, 245, 131, and 113 (Supplementary Fig. S5). Generation of m/z 131 from parent molecular ion (loss of $C_{21}H_{18}F_2N_6$; 392 Da) can be explained via Meisenheimer rearrangement. This involves temperature driven rearrangement of tertiary N-oxides into N-alkoxyamines during fragmentation [23]. Formation of m/z 113 from m/z 131 was done via loss of 18 Da indicating removal of H_2O . The product ion having m/z 477 was obtained from m/z 505 due to the loss of the ethyl group attached to the piperazine ring through heterolytic cleavage. Another fragment with m/z 421 (radical cation) was found to be formed from m/z 477 via breaking of piperazine ring. The rest of the fragments were same as shown in the fragmentation of the drug. MS3 analysis of m/z 131 revealed formation of m/z 113 due to loss of water molecule. This data support meisenheimer rearrangement in DP2 with subsequent water loss (Supplementary Fig. S9c). The mechanism behind the formation of oxidative DP2 from ABM involves a two-step process. The first step of the reaction involves the attack of piperazine nitrogen on hydrogen peroxide with its lone pair electrons leading to formation of N-OH bond and breaking weak O-O bond. In the second step this NO-H bond is getting cleaved to form DP2 (4-ethyl-1-((6-((5-fluoro-4-(4-fluoro-1-isopropyl-2-methyl-1 H-benzo[d]imidazol-6-yl) pyrimidin-2-yl) amino) pyridin-3-yl) methyl) piperazine 1-oxide) and water as a byproduct (Fig. 4) [9,24]. DP2 was also formed in small amount under photolytic condition and this can due to presence of dissolved oxygen in the reaction medium. Kalaria et al. have reported one study on characterization of hydrolytic and oxidative DPs of vilazodone through LC-ESI-MS/MS and APCI-MS. The authors have reported similar mechanism behind formation of N-oxide DP of vilazodone in peroxide based oxidative conditions [23].

3.3.2.3. Photolytic DP (DP3). The DP3 was obtained after the photolytic degradation of ABM. HPLC analysis of photolytic samples revealed retention time of DP3 as 12 min (Figs. 2h and 2i). LC-MS/MS analysis of DP3 demonstrated its protonated molecular ion peak $[M+H]^+$ at m/z 411. The possible elemental formula for DP3 was found to be $C_{21}H_{21}F_2N_6O^+$. MS/MS spectrum of DP3 depicted major fragments at m/z of 411, 395, 369, 351, 339, 324, 245, 220, 176, 149, and 108 (Fig. 3d). The calculated mass ppm error of DP3 and its major fragment ions was found to be less than 10 ppm except for the fragment with m/z 176, where the mass ppm error was found to be -11.4 (Table S6). The product ions with m/z 395 and 369 were obtained after removal of prop-1-ene and methylene groups through heterolytic cleavage, respectively (Supplementary Fig. S6). Furthermore, fragments with m/z 351 and m/z 339 were generated by subsequent removal of H_2O and HCHO from m/z 369. Two fragments with m/z 324 and m/z 245 were formed from m/z

339 via contraction of pyridine ring and heterolytical removal of 2-aminoypyridine group respectively. The fragment with m/z 245 undergoes subsequent fragmentation, leading to the formation of m/z 220 and m/z 176 through expulsion of HCN and C_2HF moieties from pyrimidine ring. MS³ analysis revealed that, fragment with m/z 245 was also produced from m/z 395 with removal of $-C_8H_{10}N_2O$ group (Supplementary Fig. S10a). The most plausible mechanistic explanation behind formation of DP3 can be hydroxylation at methyl group attached to piperazine ring followed by N-dealkylation of hydroxylated intermediate to cleave C-N bond to generated DP3 as (6-((5-fluoro-4-(4-fluoro-1-isopropyl-2-methyl-1 H-benzo[d]imidazol-6-yl) pyrimidin-2-yl) methyl) pyridin-3-yl) methanol (Fig. 4). Nord et al. reported a study on photochemical degradation of chloroquine through HRMS and NMR, the authors have discussed a similar mechanism for chloroquine photodegradation [25].

3.3.2.4. Photolytic DP (DP4). DP4 was formed under photolytic conditions (UV and Vis) and was eluted at an RT of 16.7 min during HPLC analysis (Fig. 2h and 2i). ESI-MS/MS data of DP4 depicted the quasi-molecular ion peak at m/z 425 as $[M+H]^+$ with a proposed elemental composition of $C_{21}H_{19}F_2N_6O_2^+$ (Table S6). The product ions with m/z 383, 337, 319, 310, 262, 245, 122, and 78 were obtained by ESI-MS/MS data of DP4 (Fig. 3e). A fragment with m/z 383 indicated loss of pro-1-ene group from parent ion by heterolytic cleavage which further fragmented into m/z 365 and 337 with loss of a water molecule and formic acid by heterolytic cleavage, respectively (Supplementary Fig. S7). The product ion at m/z 262 was observed from m/z 365 and 337 after heterolytic cleavage. Further, m/z 245 was formed from m/z 262 with the loss of amine group. The product ions having m/z 310 were formed from m/z 337 by ring contraction of pyridine ring through expulsion of HCN. The m/z 122 was obtained from molecular ion with a loss of $-C_{15}H_{15}F_2N_5$ group by heterolytic cleavage. CO_2 was removed from m/z 122 to give product ion with m/z 78. MS³ analysis of m/z 383 also revealed formation of fragments m/z 262 and m/z 245 with the loss of $-C_6H_3NO_2$ and $-C_6H_6N_2O_2$, respectively (Supplementary Fig. S10b). The most possible mechanism behind formation of DP4 was conversion of ABM into an amide intermediate under influence of photolytic conditions, followed by hydrolysis to form 6-((5-fluoro-4-(4-fluoro-1-isopropyl-2-methyl-1 H-benzo[d]imidazol-6-yl) pyrimidin-2-yl) methyl) nicotinic acid (Fig. 4). Bhangare et al. published one study on characterization of degradation product of capmatinib using LC-MS/MS. Authors reported similar mechanism behind formation of the DP [11].

3.3.2.5. Photolytic DP (DP5). ABM was subjected to photolytic stress, resulting in the formation of DP5. HPLC analysis showed DP5 eluted at 18.1 min (Fig. 2h and 2i). Following this, LC-MS analysis was carried out on the same sample to find out the molecular mass and elemental composition of DP5. The elemental composition of DP5 was found to be $C_{21}H_{19}F_2N_6O^+$ with m/z 409 $[M+H]^+$ (Table S6). MS/MS spectrum of DP5 exhibited fragments at m/z 409, 367, 339, 245, 220, 193, 176, 123, 106, and 78 (Fig. 3f). The mass ppm errors of all the fragments were less than 10 ppm (Table S6). A fragment with m/z 123 was generated from molecular ion with a mass difference of 286 indicated removal of $C_{15}H_{12}F_2N_4$ group via heterolytic cleavage. The removal of prop-1-ene group from the molecular ion with m/z 409 resulted in the formation of a fragment ion with m/z 367 (Supplementary Fig. S8). Subsequent loss of the amine group (-NH₃) and carbon monoxide (CO) led to generation of fragment ions with m/z 106 and 78 from m/z 123. A fragment with m/z of 339 was also formed in a similar manner through removal of -CO from m/z of 367. This fragment was further broken down to form m/z 245 and m/z 176 with expulsion of amino pyridine ring via heterolytic cleavage and contraction of pyridine ring respectively. The fragment having m/z 245 was eventually broken up into m/z 193 and m/z 220. MS³ analysis of m/z 367 also revealed formation of fragments m/z 245 and m/z 123 with removal of $-C_6H_6N_2O$ and $-C_{12}H_5N_4$, respectively (Supplementary Fig. S10c). Fig. 4 presents the proposed mechanism for

the formation of DP5. It is believed to originate from a free radical-mediated N-dealkylation of tertiary amine. This process involves the UV-induced ejection of an electron from the lone pair of the tertiary amine nitrogen, leading to the formation of an amine radical cation. Subsequently, in the presence of light, the α -carbon undergoes deprotonation facilitated by superoxide anion. The resulting radical is further oxidized, generating an iminium ion, which, upon hydrolysis, gives rise to DP5 (6-((5-fluoro-4-(4-fluoro-1-isopropyl-2-methyl-1 H-benzo [d] imidazol-6-yl) pyrimidin-2-yl) amino) nicotinaldehyde) as the N-dealkylation product of ABM [26]. Chadha R. et al. have studied characterization of stress degradation products of duloxetine. Author mentioned similar mechanism reported in this article behind formation of DP5 in photolytic conditions [27].

3.3.3. N-oxide confirmation of DP2 using APCI

It is difficult to differentiate between an N-oxide with hydroxylated product with same mass through ESI-MS spectrum. It is well reported that when N-oxide is subjected to ionization in APCI mode with high capillary temperature, it undergoes thermolytic dissociation of oxygen from the N-oxide leading to production of a characteristic peak at $M+H-16$. Fig. 5 demonstrates the mass spectrum (MS scan) of DP2 after ionization in different sources (ESI vs APCI). ESI-MS spectrum of DP2 (Fig. 5a) exhibited intact mass at m/z 523 with a prominent ion at m/z 262 ($z = 2$). When the DP2 was subjected to APCI-MS experiment, an additional peak at m/z 507 was observed as a prominent ion instead of m/z 523 indicating mass difference of 16 Da due to loss of oxygen atom attached to tertiary nitrogen of piperazine ring of DP2 (Fig. 5b). It was confirmed from this experiment that DP2 was N-oxide and not hydroxylation product of ABM.

3.4. Isolation and characterization of DP2 by 1H NMR

Isolation of DP2 was performed on HPLC to confirm its structure through other orthogonal techniques. 5 mg (4 times) of the drug was subjected to oxidative stress with 3% H_2O_2 for 15 min and the conversion of DP2 was accessed through HPLC at 100 ppm. The chromatogram revealed that a maximum of 20% of the drug was converted to DP2. Consequently, the reaction mixture was processed as discussed in procedure and DP2 was isolated. Further, for detailed analysis of DP2 structure, it was subjected to 1H NMR experiment. For evaluating alteration in structural features of DP, its NMR was compared with that of ABM. Table 1 illustrate chemical shift value (δ ppm) and multiplicity of different protons in DP2 and drug. 1H NMR spectra of DP2 and drug denoted equal numbers of protons indicated neither addition nor removal of any protons from drug's structure (Fig. 6a & b). Moreover, the chemical shift value of all protons in DP2 remained same as that of drug except H7. A downfield shift was observed for H7 proton resulting from attachment of electronegative atom (oxygen) to neighboring atom (N-8). From overall 1H NMR data, structure of DP2 was confirmed as 4-ethyl-1-((6-((5-fluoro-4-(4-fluoro-1-isopropyl-2-methyl-1 H-benzo[d] imidazol-6-yl) pyrimidin-2-yl) amino) pyridin-3-yl) methyl) piperazine 1-oxide.

3.5. In silico toxicity prediction with ProTox II software

An *in-silico* toxicity study was conducted using ProTox II software. In this, molecules are categorized into 6 different toxicity classes based on the predicted toxic dose (LD50). Class 1 molecules are considered highly toxic, while class 6 molecules are considered the least toxic. ABM is categorized under class 4 and has an estimated LD50 value of 2000 mg/kg. As per the predicted toxicity report, ABM was not found to produce any toxicity such as hepatotoxicity, cytotoxicity, carcinogenicity, or mutagenicity. The finding indicates that it doesn't interact with any potential toxicity-alarming target. All DPs were categorized in class 4. The toxicity report for all DPs generated by this software provided a confidence score for each DP. With a confidence level of **0.69** (69%) and

0.87 (87%), DP1 (O1) and DP2 (O2) were discovered to be immunotoxic. DP3, DP4 and DP5 were associated with hepatotoxicity, with confidence levels of 0.55 (55%), 0.66 (66%), and 0.62 (62%) respectively. Additionally, DP3 and DP5 were found to be associated with mutagenicity with confidence scores of 0.55 (55%) and 0.68 (68%). Table 2 depicts *in silico* toxicity report of drug and its DPs for various toxicities.

4. Conclusion

ABM demonstrated good stability under hydrolytic and thermal degradation conditions. The drug was found to degrade extensively in photolytic and oxidative stress conditions. In the present study, five new degradation products of ABM were identified and characterized through various orthogonal techniques. Among these five DPs, DP1, DP2, DP3, DP4 and DP5 were characterized employing LC-MS/MS technique. Additionally, DP2 was further characterized by using 1H NMR spectroscopy and APCI-MS to discriminate N-oxide from hydroxylated DP. A detailed degradation pathway of ABM was established with a possible mechanistic explanation behind the formation of each degradation product. The outcome of this study will be very useful for establishing more efficient storage conditions for ABM and improving its overall stability profile. The knowledge of degradation products can be useful in establishing the acceptance criteria of ABM as a drug substance or drug product during quality control and stability assessment. The developed stability indicating analytical method will be useful for pharma companies and laboratories to analyze stability samples of ABM. *In silico* toxicity study revealed that DP2-DP5 are having the potential for hepatotoxicity and immunogenicity. On the other hand, DP1 and DP2 were found to have mutagenicity. *In silico* data analysis indicates a requirement for detailed preclinical toxicological investigation of all the potential DPs of ABM aiming at the improvement of safety profile of the drug.

CRediT authorship contribution statement

Nachiket Kathar: Data curation, Formal analysis, Investigation, Methodology, Validation, Visualization, Writing – original draft. **Niraj Rajput:** Data curation, Formal analysis, Investigation, Methodology, Validation, Visualization, Writing – original draft. **Tarang Jadav:** Investigation, Methodology, Validation, Visualization, Writing – original draft. **Pinaki Sengupta:** Conceptualization, Investigation, Project administration, Supervision, Visualization, Writing – review & editing.

Declaration of Competing Interest

The authors declare that they have no known competing financial interests or personal relationships that could have appeared to influence the work reported in this paper.

Acknowledgement

We sincerely acknowledge the support of the Department of Pharmaceuticals, Ministry of Chemicals and Fertilizers, Government of India, and National Institute of Pharmaceutical Education and Research-Ahmedabad.

Appendix A. Supporting information

Supplementary data associated with this article can be found in the online version at doi:10.1016/j.jpba.2023.115762.

References

- [1] Q.Y. Chong, Z.H. Kok, X. Xiang, A.L. Wong, W.P. Yong, G. Sethi, P.E. Lobie, L. Wang, B.C. Goh, A unique CDK4/6 inhibitor: current and future therapeutic strategies of abemaciclib, *Pharmacol. Res.* 156 (2020), 104686.
- [2] H. Hino, N. Iriyama, H. Kokuba, H. Kazama, S. Moriya, N. Takano, M. Hiramoto, S. Aizawa, K. Miyazawa, Abemaciclib induces atypical cell death in cancer cells characterized by formation of cytoplasmic vacuoles derived from lysosomes, *Cancer Sci.* 111 (6) (2020) 2132–2145.
- [3] S.P. Corona, D. Generali, Abemaciclib: a CDK4/6 inhibitor for the treatment of HR +/HER2– advanced breast cancer, *Drug Des., Dev. Ther.* (2018) 321–330.
- [4] D. Thakkar, A.S. Kate, Update on metabolism of abemaciclib: In silico, in vitro, and *in vivo* metabolite identification and characterization using high resolution mass spectrometry, *Drug Test. Anal.* 12 (3) (2020) 331–342.
- [5] S. Venkataraman, M. Manasa, Forced degradation studies: regulatory guidance, characterization of drugs, and their degradation products-a review, *Drug Invent. Today* 10 (2) (2018) 137–146.
- [6] ICH, Q1A (R2) stability testing of new drug substances and products, Ich. Harmon. Tripart. Guide (2003) 1–24.
- [7] ICH, Q1B stability testing: photostability testing of new drug substances and products, Ich. Harmon. Tripart. Guidel. (1996) 1–12.
- [8] M.K. Sharma, K. Pandey, R.P. Shah, D. Kumar, P. Sengupta, A mechanistic explanation on degradation behavior of fibanserin for identification and characterization of its potential degradants using LC-DAD/ESI/APCI-Q-TOF-MS/MS, *Microchem. J.* 167 (2021), 106281.
- [9] N. Rajput, F. Soni, A.K. Sahu, T. Jadav, S. Sharma, P. Sengupta, Degradation kinetics and characterization of major degradants of binimetinib employing liquid chromatography-high resolution mass spectrometry, *J. Pharm. Biomed. Anal.* 215 (2022), 114753.
- [10] A.K. Sahu, A. Goswami, A.S. Kate, P. Sengupta, Identification and structural characterization of potential degraded impurities of ribociclib by time of flight-tandem mass spectrometry, and their toxicity prediction, *J. Pharm. Biomed. Anal.* 197 (2021), 113933.
- [11] D. Bhangare, N. Rajput, T. Jadav, A.K. Sahu, P. Sengupta, Mechanism of capmatinib degradation in stress conditions including degradation product characterization using ultra-high-performance liquid chromatography-quadrupole-time of flight mass spectrometry and stability-indicating analytical method development, *Rapid Commun. Mass Spectrom.* 37 (1) (2023), e9417.
- [12] D.K. Singh, A. Sahu, T. Handa, M. Narayanan, S. Singh, Study of the forced degradation behavior of prasugrel hydrochloride by liquid chromatography with mass spectrometry and liquid chromatography with NMR detection and prediction of the toxicity of the characterized degradation products, *J. Sep. Sci.* 38 (17) (2015) 2995–3005.
- [13] D. Bhangare, N. Rajput, T. Jadav, A.K. Sahu, R.K. Tekade, P. Sengupta, Systematic strategies for degradation kinetic study of pharmaceuticals: an issue of utmost importance concerning current stability analysis practices, *J. Anal. Sci. Technol.* 13 (1) (2022) 7.
- [14] M.K. Sharma, R.P. Shah, P. Sengupta, Amalgamation of stress degradation and metabolite profiling in rat urine and feces for characterization of oxidative metabolites of fibanserin using UHPLC-Q-TOF-MS/MS, H/D exchange and NMR technique, *J. Chromatogr. B* 1139 (2020), 121993.
- [15] P.S. Devrukhakar, M.S. Shankar, Degradation pathway proposal, structure elucidation, and *in silico* toxicity prediction of dapagliflozin propane diol hydrolytic degradation products, *Chromatographia* 83 (10) (2020) 1233–1245.
- [16] M. Kurmi, S. Kumar, B. Singh, S. Singh, Implementation of design of experiments for optimization of forced degradation conditions and development of a stability-indicating method for furosemide, *J. Pharm. Biomed. Anal.* 96 (2014) 135–143.
- [17] A.A. Kadi, H.W. Darwish, H.A. Abuelizz, T.A. Alsibi, M.W. Attwa, Identification of reactive intermediate formation and bioactivation pathways in Abemaciclib metabolism by LC-MS/MS: *in vitro* metabolic investigation, *R. Soc. Open Sci.* 6 (1) (2019), 181714.
- [18] L. Turković, L. Bockor, O. Ekpenyong, T. Silovski, M. Lovrić, S. Crnković, B. Nigović, M. Sertić, Development and validation of a novel LC-MS/MS method for the simultaneous determination of abemaciclib, palbociclib, ribociclib, anastrozole, letrozole, and fulvestrant in plasma samples: a prerequisite for personalized breast cancer treatment, *Pharmaceuticals* 15 (5) (2022) 614.
- [19] S. Alladi, K.R. Kumar, B. Mallikarjuna, Determination of abemaciclib in human plasma by lc-ms/ms analysis, *Eur. J. Mol. Clin. Med.* 8 (01) (2021).
- [20] S. Ma, S.K. Chowdhury, K.B. Alton, Thermally induced N-to-O rearrangement of tert-N-oxides in atmospheric pressure chemical ionization and atmospheric pressure photoionization mass spectrometry: differentiation of N-oxidation from hydroxylation and potential determination of N-oxidation site, *Anal. Chem.* 77 (11) (2005) 3676–3682.
- [21] M.C. Dumasia, P. Teale, N-deethylation and N-oxidation of etamiphylline: identification of etamiphylline-N-oxide in greyhound urine by high performance liquid chromatography-mass spectrometry, *J. Pharm. Biomed. Anal.* 36 (5) (2005) 1085–1091.
- [22] P.D. Kalariya, B. Raju, R.M. Borkar, D. Namdev, S. Gananadhamu, P.P. Nandekar, A.T. Sangamwar, R. Srinivas, Characterization of forced degradation products of ketorolac tromethamine using LC/ESI/Q/TOF/MS/MS and *in silico* toxicity prediction, *J. Mass Spectrom.* 49 (5) (2014) 380–391.
- [23] P.D. Kalariya, M.K. Talluri, P.N. Patel, R. Srinivas, Identification of hydrolytic and isomeric N-oxide degradants of vilazodone by on line LC-ESI-MS/MS and APCI-MS, *J. Pharm. Biomed. Anal.* 102 (2015) 353–365.
- [24] T. Dyakonov, A. Muir, H. Nasri, D. Toops, A. Fatmi, Isolation and characterization of cetirizine degradation product: mechanism of cetirizine oxidation, *Pharm. Res.* 27 (2010) 1318–1324.
- [25] K. Nord, J. Karlsson, H.H. Tønnesen, Photochemical stability of biologically active compounds. IV. Photochemical degradation of chloroquine, *Int. J. Pharm.* 72 (1) (1991) 11–18.
- [26] R. Chadha, A. Bali, G. Bansal, Identification and characterization of stress degradation products of dronedarone hydrochloride employing LC-UV/PDA, LC-MS/TOF and MSn studies, *J. Pharm. Biomed. Anal.* 118 (2016) 139–148.
- [27] R. Chadha, A. Bali, G. Bansal, Characterization of stress degradation products of duloxetine hydrochloride employing LC-UV/PDA and LC-MS/TOF studies, *J. Pharm. Biomed. Anal.* 121 (2016) 39–55.